Magnetic and Thermal Characterization of Core-Shell Fe-Oxide@SiO2 Nanoparticles for Hyperthermia Applications

Magnetic and Thermal Characterization of Core-Shell Fe-Oxide@SiO_2 Nanoparticles for Hyperthermia Hyperthermia Applications

Gabriele Barrera[1], Marco Coïsson[1], Federica Celegato[1], Elena S. Olivetti[1], Luca Martino[1], Ivana Miletto[2], and Paola Tiberto[1]

1 INRIM, Nanoscience and Materials Division, 10135 Torino, Italy
2 Department of Science and Technological Innovation, University of Piemonte Orientale "Amedeo Avogadro," 15121 Alessandria, Italy

***Abstract*—Nanoparticles for magnetic hyperthermia pose significant constraints in their size and composition to ensure cellular uptake and biocompatibility, while still requiring significant hysteresis losses exploitable at electromagnetic field values and intensities not exceeding safety limits for the human body. In this paper, core-shell Fe-oxide@SiO_2 nanoparticles have been synthesized, and their size has been controlled so that the blocked-to-superparamagnetic transition is close to room temperature. Their size remains, therefore, as small as possible, while still displaying significant hysteresis losses in dynamic conditions (electromagnetic fields up to 48 kA/m at 100 kHz). Static loops measured by vibrating sample magnetometry and dynamic loops measured by a custom B-H tracer are used to characterize the particles' magnetic properties, as well as a custom-built, fully modeled, hyperthermia setup. The specific absorption rate is obtained either from static and dynamic loop areas or from direct hyperthermia measurements. Dynamic loops are shown to be a good estimator of specific absorption rate values.**

***Index Terms*—Core-shell nanoparticles, hysteresis losses, magnetic hyperthermia, specific absorption rate.**

I. Introduction

Magnetic hyperthermia consists of exploiting the energy losses in magnetic nanoparticles, excited by a suitable alternating electromagnetic field, for releasing heat at a controllable rate in a given environment at a given time. If the magnetic nanoparticles can be delivered to tumor masses and either internalized or attached to tumor cells, the heat released could be exploited to kill the cells or to locally release drugs attached to the particles surface. Magnetic hyperthermia is therefore an extremely interesting potential technique for treating cancer [1].
However, this subject still presents many open issues that require expertise from different disciplines, including toxicity studies, choice of the optimum dose, understanding of the exact mechanisms that can induce cells death, development of laboratory setups giving reliable, comparable and traceable hyperthermia measurements [2], [3], and development of the most promising nanomaterials for this kind of application [4]. Given the extremely high impact that such topic can have on human society, interdisciplinary research has been active on this subject over the past few years.
In this paper, we have synthesized core-shell Fe-oxide@SiO_2 nanoparticles which combine magnetic properties to be exploited for hyperthermia applications and an inert, biocompatible shell that will allow further functionalization for targeting cancer cells [5], [6]. While small nanoparticles are often preferred because they can more easily be internalized by cells, their magnetic properties severely degrade when they reach the superparamagnetic state, characterized by negligible hysteresis losses. We have therefore tailored the Fe-oxide cores sizes to keep the blocked-to-superparamagnetic transition temperature close to room temperature, so that energy losses in typical hyperthermia conditions (magnetic fields up to 48 kA/m at 100 kHz in our laboratory conditions) are sufficiently high without requiring electromagnetic fields of excessive intensity. What resulted is a nanoparticles system that shows a nearly superparamagnetic behaviour useful for preventing agglomeration and for keeping particles size small, while keeping hysteresis losses in dynamic conditions to ensure heat generation for biomedical applications such as hyperthermia or heat-assisted drug release.

II. Methods and Procedures

Magnetic nanoparticles were synthesized by coprecipitation of iron (II) and iron (III) chlorides in alkaline water solution [7]. The produced particles were then covered with a silica shell applied by a two-step process comprising a sol-gel reaction with Tetraethoxysilane and a precipitation from a supersaturated silica solution, as described in [8]. This preparation route allowed deposition of a thin and uniform silica layer, and to avoid both homogeneous nucleation of silica (e.g., formation of SiO_2 particles) and the sintering between different nanoparticles, allowing maximization of the saturation magnetization of the nanocomposite.
High-Resolution Transmission Electron Microscopy (HRTEM) images were collected on a JEOL 3010 High Resolution Transmission Electron Microscope operating at 300 kV. For the measurements, samples were dispersed in isopropanol and sonicated; few drops of the suspension were then deposited on carbon-coated grids. The average size of

Fe-oxide and Fe-oxide@SiO_2 was obtained by measuring ~300 particles, and the mean particle diameter (d_m) was calculated as $d_m = d_i n_i / n_i$, where n_i is the number of particles of diameter d_i. The results are indicated as ($d_m \pm STDV$).
X-Ray diffraction (XRD) was performed in Bragg-Brentano geometry with Co Kα radiation on the as prepared, uncoated particles to evaluate the crystalline quality and phase composition of the sample.
Low-temperature magnetization measurements have been performed with a superconducting quantum interference device vibrating sample magnetometer (Quantum Design MPMS SQUID-VSM3). Field-cooled (FC) and zero-field-cooled (ZFC) measurements have been performed under an applied field of 4000 A/m.
Room temperature static hysteresis loops, both major and minor, have been measured with a vibrating sample magnetometer (LakeShore VSM 7410).
Dynamic hysteresis loops have been measured at room temperature with a custom built B-H tracer [3] under the application of ac electromagnetic fields at ~69 kHz with maximum (vertex) values (H_v) up to 48 kA/m.
Hyperthermia measurements have been conducted with a custom built setup [3] under the application of ac electromagnetic fields at ~100 kHz with maximum values up to 48 kA/m. A fiber-optic thermometer has been used to measure temperature both during heating and cooling down. Heating time lasted for one hour, whereas the samples were allowed to cool down for the necessary time until room temperature was reached.
The specific absorption rate (SAR), defined as the power released by the particles per gram of particles, and measured in W/g, has been calculated in the three measured conditions. For static and dynamic loops, the loop area is measured and multiplied by the alternating field frequency (69 kHz); in the case of dynamic loops, this is of course the frequency at which the field has been cycled between the vertex field $\pm H_v$ during the measurements, whereas in the case of static loops this operation is equivalent to assume that the static loop is repeated a certain number of times (69000 in our case) each second; a power loss is therefore obtained for both kind of loops, that of course for the static loops will not take into account any dynamic effects. In the case of hyperthermia measurements, the time dependence of the water solution containing the particles is analysed with a suitable thermodynamic model [3] from which the associated SAR value is directly obtained.

III. Results and Discussion

Morphology, size and dispersion of both uncoated and SiO_2 coated magnetic nanoparticles were investigated by HRTEM analysis. In Fig. 1, representative images are reported. Pristine magnetic nanoparticles are quite uniform in shape and size, being characterized by an average diameter of 12 ± 2 nm. The deposition of a thin SiO_2 layer led to a small increase in the average diameter of the nanoparticles (14 ± 3 nm) without the formation of SiO_2 particles, as expected. As clearly visible in Fig. 1(b), magnetic nanoparticles are uniformly coated by a thin amorphous silica layer and remained monodispersed (e.g., no sintered nanoparticles were found).

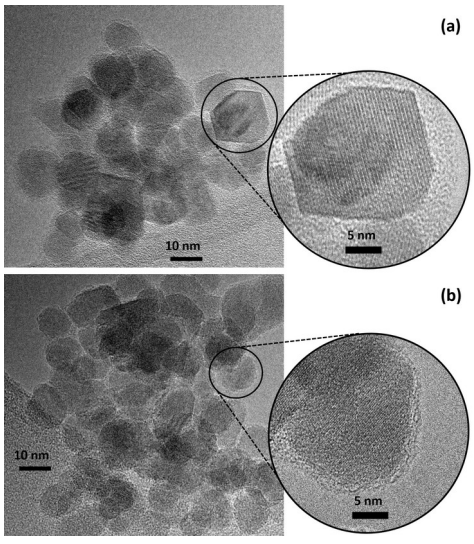

Fig. 1. HRTEM images of (a) uncoated and (b) SiO_2 coated magnetic nanoparticles.

Magnetite (Fe_3O_4) and maghemite (γ-Fe_2O_3) are two iron oxides which can be successfully synthesized in nanosized particles with simple chemical methods. They share the same inverse spinel structure with similar lattice parameters, so they exhibit very similar diffraction patterns, the only difference is the appearance of low-intensity superlattice lines (reflections with mixed Miller indices) in the cation-deficient maghemite, which do not occur in magnetite. In addition, the two oxides are known to form solid solutions with a continuous variation of the lattice constant *a* with the degree of oxidation [9]. For these reasons, their identification in an experimental XRD pattern can be tricky, especially in nanomaterials, owing to the large width and to the decreased intensity of the XRD peaks [10].

The X-ray diffraction pattern of the uncoated particles is displayed in Fig. 2: all the peaks can be indexed with a cubic unit cell with inverse spinel structure, with lattice parameter a = 8.356 A°. This value is consistent with an almost fully oxidised form of magnetite [9], with formula very close to the one of maghemite (γ-Fe_2O_3). In the following, the composition of the magnetic nanoparticles will be simply indicated as Fe-oxide.
The crystallite size, estimated through the Sherrer formula from the peak full-width-at-half-maximum after subtraction of the instrumental broadening, is 12 nm: a value in good agreement with the one obtained from TEM observations.

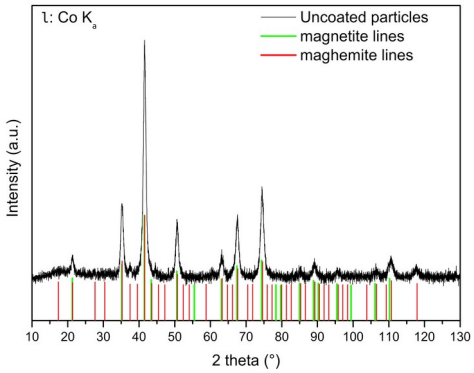

Fig. 2. XRD pattern of the uncoated, as prepared, magnetic nanoparticles. Magnetite and maghemite lines (PDF-01-088-0315 and 00-039-1346, respectively, of the ICCD database) are reported as a reference.

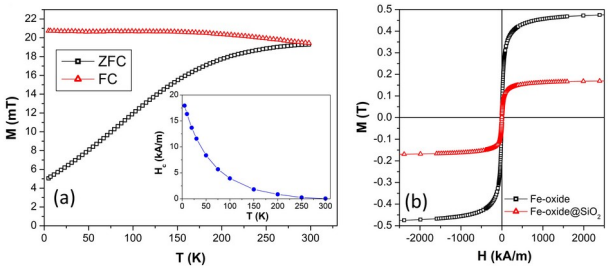

Fig. 3. (a) Field-Cooled and Zero-Field-Cooled measurements of the Feoxide@SiO2 sample under an applied field of 4000 A/m. (Inset) Evolution of the coercive field as a function of temperature. (b) Comparison of the room temperature hysteresis loops of the Fe-oxide and Fe-oxide@SiO2 samples.

FC-ZFC curves of the Fe-oxide@SiO_2 sample are shown in Fig. 3(a). The two curves merge very close to room temperature, indicating that the particles size and interactions induce a transition from the blocked to the superparmagnetic regime close to 300 K. Indeed, this is confirmed by the temperature evolution of the coercive fields (see Fig. 3(a) inset), that become almost zero at 300 K. This feature can be of interest for hyperthermia applications, where a true superparamagnetic system is not recommended, because of the extremely reduced energy losses, but also a significantly hysteretic (hard) magnetic system should be avoided, as hyperthermia applications impose severe limits on the amplitude of the alternating magnetic fields that can be applied ($5.0 \cdot 10^9$ A/ms [11]). Additionally, superparamagnetic or nearly superparamagnetic particles have an almost zero magnetic remanence, a condition usually sought for to minimize agglomeration. Fig. 3(b) compares the room temperature hysteresis loops of the Fe-oxide samples with and without SiO_2 shell. The uncoated sample presents a saturation magnetisation value very close to that of bulk maghemite (0.497 T [12]). The saturation magnetization of the uncoated sample is larger than that of the coated one, as normalization to the mass has been done in the latter case including the weight of both the Fe-oxide core and the SiO_2 shell (whose nominal densities, 5.2 and 2.65 g/cm^3 respectively, have been used in the calculations). By assuming that the Fe-oxide cores have the same saturation magnetization as the uncoated Fe-oxide particles (black squares, Fig. 3(b)) and that the magnetic contribution of the SiO_2 shell is negligible, the relative mass amounts can be estimated as 52 wt.% Fe-oxide core and 48 wt.% SiO_2 shell.

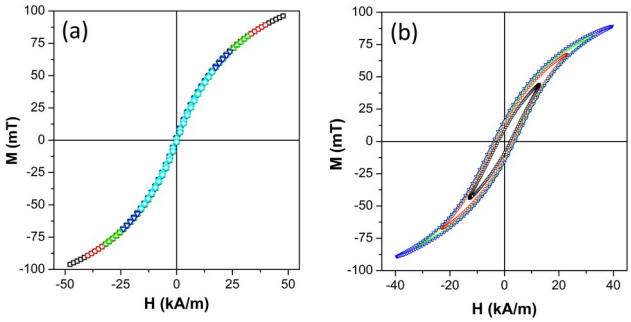

Fig. 4. (a) Static and (b) dynamic room temperature hysteresis loops of the Feoxide@SiO2 sample. Symbols with different colors represent loops measured with different vertex field values.

Room temperature hysteresis loops, both static and dynamic, of the Fe-oxide@SiO_2 sample are reported in Fig. 4. All loops have been measured at different values of the maximum (vertex) field, within the limits usually considered as acceptable for magnetic hyperthermia applications [11]. As a result, both in static and dynamic conditions, the loops are minor, i.e., they do not saturate. By comparing the static and dynamic loops, it is evident the role of frequency in determining energy losses: even though the Fe-oxide@SiO_2 particles are almost in the superparamagnetic state at room temperature (therefore static loops have almost zero hysteresis), dynamic loops at comparable vertex field values display a significant loop area. This fact may be due to the usual energy losses contributions [13]; additionally, it must be considered that the temperature at which the transition between the superparamagnetic and the blocked regimes takes place is defined through the equation $K_u V = 25\, k_B T$, where K_u is the (uniaxial) anisotropy of the particles, V is their volume, k_B is the Boltzmann constant, and T is temperature. The factor 25 takes into account the different time scales between the relaxation time of the particles magnetic moment due to thermal agitation, and the duration of the measurement [14]. While FC-ZFC measurements and VSM loops are performed in static conditions, dynamic loops are measured at a frequency oscillation of the field of 69 kHz; the duration of the measurement is therefore much shorter, and consequently, the corresponding blocking temperature at that time scale shifts towards higher values, possibly beyond room temperature where, in static conditions, the particles have just become superparamagnetic. Both effects probably contribute to the significant increase of the loops area in dynamic conditions. It is important to remark that the vertical axis of Fig. 4(b) has been calibrated assuming that the maximum magnetization value attained by the Fe-oxide@SiO_2 sample is the same in static and dynamic conditions under the application of the same vertex field. The dynamic loops data have thus been calibrated on the VSM data. This assumption is required by the complexity of the calibration process of the custom built dynamic loop tracer, but may induce a slight overestimation of the magnetization of the sample in dynamic conditions. This will be further discussed later.
The hysteresis losses responsible for the loops shown in Fig. 4(b) are therefore expected to induce heating in the Fe-oxide@SiO_2 particles. To measure their ability to heat a fluid, particles have been suspended in pure water (typical resistivity 10 MΩ cm at 25 °C) at a concentration of 10 mg/mL and hyperthermia measurements have been conducted under different applied field intensities. The time dependence of the temperature T_W of the water solution under an applied field of 40 kA/m at 100 kHz is shown in Fig. 5. This measurement is taken as representative of all measurements done at different applied field values. The alternating field is switched on at the beginning of the measurement and switched off after one hour; then, the solution is allowed to cool down to room temperature again. The black symbols are the experimental data, whereas the green line is the theoretical model [3]. From the theoretical curve, the power released by the nanoparticles can be extracted, corrected for the calibration factors and the spurious heating of the water induced by the ionic currents flowing through it. From the value of the power released by the particles, and by knowing their mass, the specific absorption rate (SAR) can be calculated as the ratio of the power and the mass.

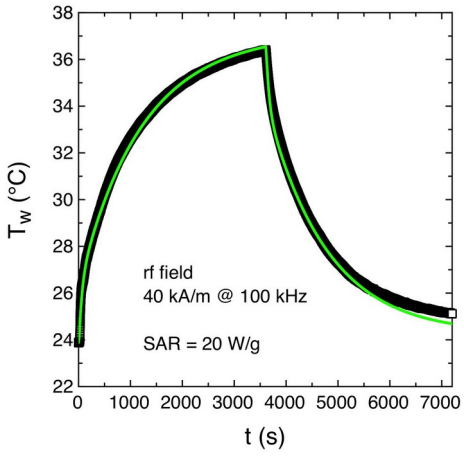

Fig. 5. Time dependence of the temperature of the water solution containing 10 mg/mL of Fe-oxide@SiO2 particles under an applied field of 40 kA/m at 100 kHz. Black symbols: experimental data. Green line: theoretical model after [3].

The SAR of the Fe-oxide@SiO_2 particles is therefore reported in Fig. 6, as obtained from the three different measurements presented above in Figs. 4 and 5: static loops, dynamic loops and hyperthermia. In Fig. 6, all data have been normalized to either the total mass of the core/shell system, or to the mass of the Fe-oxide cores alone (see the left and right vertical axes of Fig. 6 respectively). Static losses (see the squares in Fig. 6) are negligible, given the extremely reduced coercivity of the VSM loops for these samples (see Fig. 4(a)). Conversely, dynamic losses (see the triangles in

Fig. 6) are significantly improved, as discussed earlier (see Fig. 4(b)). SAR values obtained from hyperthermia measurements (see the diamonds in Fig. 6) are slightly lower than those obtained through dynamic loops measurements.

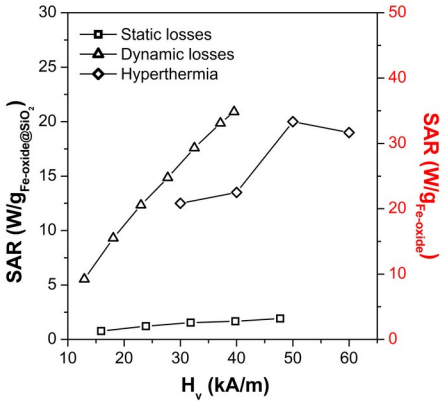

Fig. 6. Specific absorption rate (SAR) of the Fe-oxide@SiO2 particles as a function of the maximum (vertex) alternating field Hv measured from static loops area (squares), dynamic loops areas (triangles), and hyperthermia measurements (diamonds). SAR is calculated by normalizing to either the total mass of the Fe-oxide@SiO2 core/shell particles (left vertical axis) or the mass of the Fe-oxide cores (right vertical axis).

This small discrepancy is due to a number of factors, which include the fact that during the two measurements the samples are not in the same conditions. In fact, hyperthermia is measured on water dispersions of the particles, whereas dynamic loops are measured on dry, compacted powders; this difference is due to the fact that the weaker signal in a water-dispersed sample turned out to be too much affected by noise, therefore forcing us to measure dynamic loops only on dry powders. Additionally, the magnetization measured with dynamic loops has been calibrated with the method described earlier, and could be slightly overestimated. Finally, we have to keep in mind that small differences between the two sets of data can also be attributed to the slightly different working frequencies of hyperthermia and dynamic loops (100 kHz and 69 kHz, respectively), and to the different role played by inter-particle interactions in the two diluted and dry particles samples [15]. We can therefore conclude that the SAR values obtained from dynamic loops and hyperthermia measurements are comparable within the experimental uncertainties, whose exact values are currently under evaluation.

IV. Conclusion

Core-shell Fe-oxide@SiO_2 nanoparticles having a blocked-to-superparamagnetic transition temperature close to 300 K have been prepared and characterized for hyperthermia applications. While static energy losses are negligible as the nanoparticles are almost superparamagnetic at room temperature, dynamic energy losses contribute to the ability of these core-shell particles to heat water solutions under the application of ac magnetic fields at ~100 kHz with intensities up to 48 kA/m. Dynamic hysteresis loops, in spite of the complexity of calibration of B-H tracers built for this purpose, have been shown to be good estimators of SAR values.

References

[1] S.Dutz and R. Hergt, “Magnetic particle hyperthermia–A promising tumor therapy?” *Nanotechnology*, vol. 25, 2014, Art. no. 452001.
[2] RADIOMAG COST action, Newsletter, Aug. 2016. [Online]. Available: http://www.cost-radiomag.eu/News/RADIOMAG-newsletter-Augustissue_1
[3] M. Coïsson *et al.*, “Hysteresis losses and specific absorption rate measurements in magnetic nanoparticles for hyperthermia applications” *BBA Gen. Subjects*, vol. 1861, pp. 1545–1558, 2017.
[4] E. Pollert and K. Zaveta, “Nanocrystalline oxides in magnetic fluid hyperthermia” in *Magnetic Nanoparticles: From Fabrication to Clinical Applications*, N. T. K. Thanh, Ed. Boca Raton, FL, USA: CRC, 2012, pp. 449–477.
[5] A. K. Gupta and M. Gupta, “Synthesis and surface engineering of iron oxide nanoparticles for biomedical applications,” *Biomaterials*, vol. 26, pp. 3995–4021, 2005.
[6] L. Ansari and B. Malaekeh-Nikouei, “Magnetic silica nanocomposites for magnetic hyperthermia applications,” *Int. J. Hyperthermia*, vol. 33, no. 3, pp. 354–363, 2017.
[7] I. J. Bruce *et al.*, “Synthesis, characterisation and application of silica-magnetite nanocomposites,” *J. Magn. Magn. Mater.*, vol. 284, pp. 145–160, 2004.
[8] Q. Liu, Z.Xu, J. A. Finch, and R. Egerton, “A novel two-step silica-coating process for engineering magnetic nanocomposites,” *Chem.Mater.*, vol. 10, pp. 3936–3940, 1998.
[9] D. J. Dunlop and Ö. Özdemir, *Rock Magnetism*. Cambridge, U.K.: Cambridge Univ. Press, 1997.
[10] D. Ortega, *Magnetic Nanoparticles: From Fabrication to Clinical Applications*, N. T. K. Thanh, Ed. Boca Raton, FL, USA: CRC, 2012, pp. 10–11.

[11] R. Hergt, S. Dutz, and M. Zeisberger, “Validity limits of the Neel relaxation model of magnetic nanoparticles for hyperthermia,” *Nanotechnology*, vol. 21, 2010, Art. no. 015706.
[12] D. Cao *et al.*, “High saturation magnetization of γ-Fe_2O_3 nano-particles by a facile one-step synthesis approach,” *Sci. Rep.*, vol. 6, 2016, Art. no. 32360.
[13] C. Beatrice, V. Tsakaloudi, S. Dob´ak, V. Zaspalis, and F. Fiorillo, “Magnetic losses versus sintering treatment in Mn-Zn ferrites,” *J. Magn. Magn.Mater.*, vol. 429, pp. 129–137, 2017.
[14] B.D. Cullity and C.D. Graham, *Introduction to Magnetic Materials*.Hoboken, NJ, USA: Wiley, 2009.
[15] I. Conde-Leboran *et al.*, “A single picture explains diversity of hyperthermia response of magnetic nanoparticles,” *J. Phys. Chem. C*, vol. 119, no. 27, pp. 15698–15706, 2015.